Dominik Junger, Marco Liebscher, Jitong Zhao, Viktor Mechtcherine

Joule heating as a smart approach in enhancing early strength development of mineral-impregnated carbon-fibre composites (MCF) made with geopolymer

Erstveröffentlichung in / First published in:

Composites : Part A, Applied science and manufacturing. 2022, 153, 106750. {Zugriff am: 01.03.2023}. Elsevier. ISSN 1359-835X.

DOI: https://doi.org/10.1016/j.compositesa.2021.106750

Final edited form was published in "Composites : Part A, Applied science and manufacturing" 153,106750. ISSN: 1359-835X
https://doi.org/10.1016/j.compositesa.2021.106750

Joule heating as a smart approach in enhancing early strength development of mineral-impregnated carbon-fibre composites (MCF) made with geopolymer

Dominik Junger, Marco Liebscher *, Jitong Zhao, Viktor Mechtcherine

Technische Universitat Dresden, Institute of Construction Materials, 01062 Dresden, Germany

ARTICLE INFO

Keywords:
Carbon-fibre composites
Automated processing
Pultrusion
Mechanical testing
Joule heating

ABSTRACT

The article at hand presents a novel approach to accelerating the early strength development of mineral-impregnated carbon-fibre composites (MCF) by electrical Joule heating. MCF were produced with a metakaolin-based geopolymer suspension and subsequently cured using Ohmic heating under systemically varied voltages and durations.

The MCF produced were characterised in respect of their mechanical and morphological properties. Three-point-bending and uniaxial tension tests yielded significant enhancement of MCF mechanical properties due to curing within only a few hours. Thermogravimetric analysis (TGA), mercury intrusion porosimetry (MIP), environmental scanning electron microscope (ESEM) as well as micro-computed tomography (μCT) confirmed advanced geopolymerisation by the electrical heating process and a strong sensitivity to parameter selection. After only two hours of resistance heating MCF could demonstrate tensile strength of up to 2800 MPa, showing the great potential for applying the Joule effect as a possibility to enhance the strength development of geopolymer-based MCF. Moreover, the applied method offers a huge potential to manufacture automated fast out-of-oven cured MCF with a variety of shapes and dimensions.

1. Introduction

Owed to its energy and resource-intensive production, cement accounts for a very large share of CO_2 emission. In conventional steel-reinforced concrete, a high amount of cement is required just to ensure sufficient coverage of the steel rebar to prevent it from corroding. Hence, there is a need to find alternative reinforcing materials to reduce material consumption and the emission of greenhouse gases and to increase the durability of structural members.

Here, carbon fibres (CF) represent a promising reinforcement type due to their high tensile strength, corrosion resistance, and low density [1,2]. With these advantages only thin concrete covers are required and, hence, very slender, resource-saving structural components can be constructed. For applications in civil engineering, the CF reinforcements usually consist of unidirectional multifilament CF yarns bundled as bars or textiles and embedded in thermosetting or thermoplastic matrices, also known as carbon-fibre reinforced polymers (CFRP). The polymeric matrices exhibit good force transfer from their outer filaments to their inner filaments, thus maximizing the load-bearing of the fibre reinforcement [3,4]. However, such polymer-based composites show weak chemical bonding towards mineral matrices as well as poor mechanical behaviour at elevated temperatures as a consequence of their softening behaviour and thermal decomposition [5-8]. This leads both to a reduction in bond strength between the CF and the surrounding concrete matrix and to a decrease in the CFRPs' strength, thus considerably limiting the application range of the CFRP-reinforced concrete in construction [9-11].

To solve this problem, a mineral-based matrix on a basis of micro-cement has been developed to produce so-called mineral-based carbon fibre composites (MCF), a novel group of materials showing significantly higher thermal stability and better bond behaviour [12,13]. Schneider *et al.* [13] reported adequate bond behaviour even at temperatures up to 500 °C. Moreover, this newly developed reinforcement type shows high potential for direct integration into emerging concrete technologies, such as 3D concrete printing [14,15]. However, the cement-based suspensions can be given only insufficient processing time for continuous industrial production since the viscosity of the cement slurry increases quickly due to its successive hydration [14]. This results in a very limited

* Corresponding author.
E-mail address: marco.liebscher@tu-dresden.de (M. Liebscher).

https://doi.org/10.1016/j.compositesa.2021.106750
Received 7 June 2021; Received in revised form 17 September 2021; Accepted 27 November 2021
Available online 2 December 2021

Final edited form was published in "Composites : Part A, Applied science and manufacturing" 153,106750. ISSN: 1359-835X
https://doi.org/10.1016/j.compositesa.2021.106750

process window for the efficient impregnation of the CF yarns with such cement-based slurries. Furthermore, after the impregnating process the cement-based composites commonly need several weeks to gain sufficient stiffness and strength.

Geopolymer (GP) binders represent a very promising alternative in this regard due to their long-lasting processability in early stages, excellent thermal stability over a wide temperature range, and high strength. These binders – based, for instance, on metakaolin or fly ash as precursor – can form a solid structure within short periods when being thermally treated, by means of a significant acceleration in their chemical reactions [16,17].

To date most studies have focused on geopolymer composites with short fibres for achieving better mechanical characteristics when exposed to high temperatures [18,19]. Only a few studies reported on continuous carbon-fibre reinforcements with geopolymer [20-22]. Tran *et al.* [21,22] produced fibre reinforced geopolymer composites using a CF yarn with 24,000 single filaments and a fineness of 1,600 tex, achieving a flexural strength of 570 MPa after curing the composite at 75 °C. Zhao *et al.* [23] produced MCF in a continuous automated processing line with a metakaolin-based suspension, which gained rapid early-strength development by subsequent oven curing at 75 °C within several hours.

Common processes for the thermal treatment of mineral-based materials use an oven, autoclave, or steam [24-26]. However, those methods demand high energy, and the specimens are heated from outside to inside, which requires more time to form a solid aluminosilicate structure of geopolymers, which are sensitive to water loss.

Since MCF are electrically conductive to a considerable degree, Joule heating presents itself as a great opportunity to reduce the curing duration of such samples by providing electric energy via the CF. The induced electrical field causes a movement of charge-carriers through the specimen in the fibres' direction, enabling a collision of charge-carriers with each other and with atoms of the electrical conductor. These collisions dissipate energy in the form of heat [27] which can be used to accelerate the geopolymerisation.

The resulting electrical power (P) and the emitted heat (Q) during such an electrical process can be calculated using Eqs. (1) and (2):

$$P \quad U^2/R \tag{1}$$

and

$$Q \quad P \cdot t \quad (U^2/R) \cdot t \tag{2}$$

where U is the voltage, R the resistance, and t the time.

As can be seen, an increase in voltage results in an increase in the heat emitted when keeping the dimensions of the samples constant.

Kovtun *et al.* [28] and Ziolkowski and Kovtun [29,30] applied Ohmic heating on fly ash-based geopolymers. Direct electric curing for only 7 min resulted in high early and 28-day strengths of 11.5 MPa and 20.1 MPa, respectively [29,30]. Cai *et al.* [31] added both carbon black and steel fibres to develop an electrically conductive network in fly-ash-based geopolymer and achieved maximum compression forces of up to 1.7 kN after two hours of curing and 7 days of storing, as compared to 0.7 kN measured for the specimens cured in the standard laboratory environment due to more pronounced dissolution of the fly ash particles and, therefore, a denser matrix. Tian *et al.* [32] demonstrated the possibility to cure fly ash-blended concrete pavements in severely cold regions (-20 °C), achieving similar strengths to those of the references cured at room temperature for 3 days.

Besides the thermal curing of materials, Joule heating is also reported as an appropriate solution for de-icing concrete pavements [33-39]. For CFRPs, resistance heating has been mainly investigated to treat so-called prepregs, i.e. pre-impregnated, non-cured carbon fibre composites, in order to melt the polymers and gain a solid structure [40-45]. Recently, also out-of-oven and out-of-autoclave curing was reported for Joule heating as an energy-efficient method to harden composites with complex shapes [46-48].

In the present investigation an innovative approach is followed by manufacturing MCF in an automated and continuous impregnation process plus a subsequent controlled internal thermal treatment by means of Joule heating to accelerate the geopolymerisation. Due to the easy handling and flexibility compared to oven or steam curing, this method is also believed to be an auspicious possibility to enable the deployment of MCF on the construction site.

2. Experimental program

2.1. Materials

Metakaolin (MK), MetaMax® from BASF, Germany, was used as the aluminosilicate source for the geopolymer binder due to its high reactivity and small average particle size of 1.3 μm. Note that particle sizes smaller than the filament diameter are usually required to achieve the optimal fibre–matrix distribution and stable impregnation process [14]. Potassium silicate solution Geosil 14517 from Woellner, Germany, with a solid content of 45%, and a SiO_2/K_2O molar ratio of 1.7 was used as the alkaline activator. Sapetin D27, based on phosphonic acids modified by salts from Woellner, Germany, was used as superplasticizer (SP) with a dosage of 4% by mass of the GP to attain the required flowability for the impregnation process. The mix design, based on a previous study [49], is given in Table 1.

The carbon fibre roving under investigation was SIGRAFIL® C T50-4.4/255-E100 from SGL Carbon, Germany. It consisted of 50,000 individual filaments, each having a diameter of 6.9 μm and specific resistance of 17 μΩm. The yarns have tensile strength and Young's modulus of 4.4 GPa and 255 GPa, respectively. Additional technical data as provided by the manufacturer is given in Table 2.

2.2. Fabrication of MCF

The impregnating suspension was prepared by mixing the MK powder with the potassium silicate solution and the SP. The mixing process was divided into the following steps, suggested previously in [23]: (I) mixing the suspension for two minutes at 7000 rpm with a high-speed disperser IKA® T50 digital ULTRA TURAXX®, (II) addition of the SP, (III) mixing the suspension for another six minutes to ensure the full dispersion of metakaolin particles, (IV) vibration of the mixture for ten minutes to remove air bubbles.

A continuous, automated pultrusion device, described in detail in [23], was used to impregnate the carbon yarns with the geopolymer suspension. During the impregnating process, the carbon-fibre yarn was pulled through a five-roller foulard by rotating a hexagonal wheel driven by an electric motor at a pulling speed of 360 m/h and then past one nozzle with a diameter of 4.5 mm to take off excess suspension followed by two nozzles of diameter 4.1 mm placed downstream, each for final shaping of the MCF. Finally, the freshly impregnated yarn elements were regularly placed on a circulating wheel with a constant segment length of 1.2 m, making six segments per rotation of the wheel.

2.3. Post-treatment by Joule heating

After initial impregnation, the fresh MCF were cut into pieces, each of 1.2 m length. Their ends were washed with tap water and dried with

Table 1
Composition of metakaolin-based geopolymer impregnation suspension.

Metakaolin MetaMax®	1000.0 kg/m^3
Water glass Geosil 14517	549.3 kg/m^3
Sapetin D27	62.0 kg/m^3
WG/MK ratio	1.86

Final edited form was published in "Composites : Part A, Applied science and manufacturing" 153,106750. ISSN: 1359-835X
https://doi.org/10.1016/j.compositesa.2021.106750

Table 2
Technical data of SIGRAFIL® C T50-4.4/255-E100 .

Number of filaments	50,000
Fineness of the yarn	3,450 tex
Density	1.8 g/cm^3
Filament Diameter	6.9 µm
Filament tensile strength	4.4 GPa
Filament modulus of elasticity	255 GPa
Sizing type	Epoxy
Sizing degree	1.0 %

paper towels before connecting the electrode via alligator clamps. To reduce the contact resistance between the clamps and the yarns, a silver paste, ACHESON 1415 from PLANO, Germany, was applied to the fibre's surfaces. Subsequently, the freshly impregnated yarns were hung vertically and loaded with small weights of 50 g each to keep their nearly circular cross-sectional shape and to avoid any twisting caused by fixing the clamps. Afterwards, the electrodes were connected at a distance of 1.0 m.

The Joule heat curing process was conducted by using the power supplies Voltcraft LPS1305 and PeakTech 6015 A. The process parameters under investigation are shown in Table 3. During the treatment, temperature was recorded in the middle of the yarns by using a FLUKE 289 multimeter with a temperature sensor connected to a computer, as shown in Fig. 1.

2.4. Flexural tests

To determine flexural properties as an indicator for the quality of the impregnation and curing processes, three-point bending tests were performed using a ZwickiLine Z2.5 from ZwickRoell, Germany with a load cell capacity of 2.5 kN, a displacement rate of 5 mm/min, and a support span of 100 mm. For each curing combination, six specimens were tested.

To calculate the flexural strength of each yarn, which was considered to have an elliptical shape, the height (h) and width (b) of the cross-sections were measured individually. The maximum flexural stress was calculated as follows:

$$\sigma_{max} \quad \frac{8FL}{\pi bh^2} \tag{3}$$

where F is the maximum force and L is the support span.

The bending tests were performed immediately after curing via Ohmic heating as well as at an age of 28 days. All samples were sealed with plastic foil and stored at 20 °C and 55% relative humidity until testing.

2.5. Uniaxial tension tests on yarns

To investigate the tensile behaviour of the MCF, uniaxial tension tests were carried out using a hydraulic mechanical testing machine EU 20 in accordance with ISO 10406–1 [50]. The ends of the specimen, with a total length of 600 mm, were anchored in 100 mm long aluminum tubes (Fig. 2) and cast with epoxy resin to avoid damaging the MCF due to transverse stress concentrations from clamping.

Elongation was measured by using an electro-optical video-extensometer Rudolph XR200 with a gauge length of 100 mm placed in the middle of the specimens. For this purpose, black- and white-striped measuring marks were glued onto the surfaces of the yarns; see Fig. 2. Details of the test set-up can be seen elsewhere [23].

Table 3
Chosen parameters for the Joule heating experiment.

Voltage [V]	Curing duration [h]
7.5	0.25
15	0.5
30	1.0
	2.0

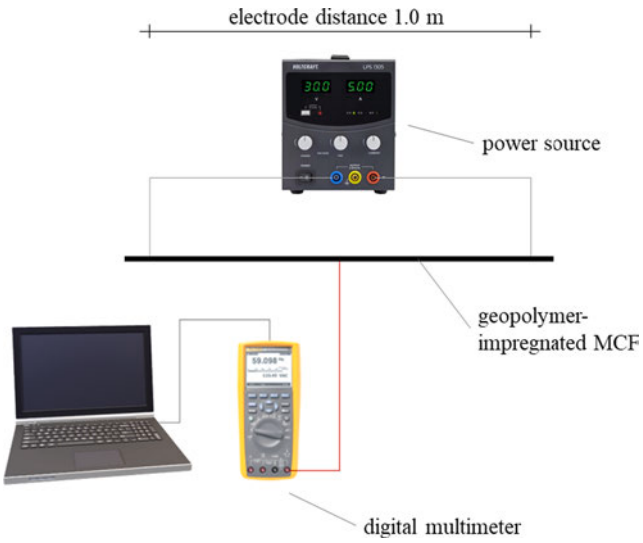

Fig. 1. Experimental setup for Joule heating of MCF.

The tensile strength of the MCF is calculated by dividing the maximum force of each specimen by the sum of the cross-sections of every single filament, the procedure commonly used in characterising carbon-textile reinforced concrete [51]. Hence, the tensile strength is determined following Eq. (4):

$$\sigma_{max} \quad \frac{F}{50000 \bullet \pi \bullet r_{CF}^2} \tag{4}$$

where F is the maximum tensile force and r_{CF} is the radius of each single CF-filament.

The modulus of elasticity was determined as follows:

$$E \quad \frac{0,7\sigma_{max} \quad 0,2\sigma_{max}}{\varepsilon_{0,7\sigma_{max}} \quad \varepsilon_{0,2\sigma_{max}}} \tag{5}$$

Note, due to the excessive sample preparation, the tensile tests were conducted 2 days and 28 days subsequent to the impregnation and heating processes. Moreover, MCF without any thermal treatment were tested at the specimens' age of 28 days as a control and compared with the thermally treated MCF.

2.6. Morphological and analytical characterization

The microstructure of the composites was analysed by using an environmental scanning electron microscope (ESEM) Quanta 250 FEG from FEI, Eindhoven, The Netherlands. In addition, µCT-scans were performed to characterise the structure of the geopolymer-impregnated carbon-fibre yarns without damaging them by using a CT-XPRESS from ProCon X-Ray, Germany, at a voltage and amperage of 72 kV and 200 mA, respectively. To assess the porosity and pore-size distribution of the composites, mercury intrusion porosimetry (MIP) was performed utilizing a Porotec porosimeter PASCAL 140/440 with a pressure range from 0.00 MPa to 400.71 MPa. Thermogravimetric analysis (TGA) was conducted by using a thermal system STA 409 from Netzsch, Germany. During the analysis, the samples were heated to 1000 °C under an oxygen atmosphere at a heating rate of 10 K/min. Before testing, all samples were stored in *iso*-propanol for at least 24 h to remove free pore water.

Final edited form was published in "Composites : Part A, Applied science and manufacturing" 153,106750. ISSN: 1359-835X
https://doi.org/10.1016/j.compositesa.2021.106750

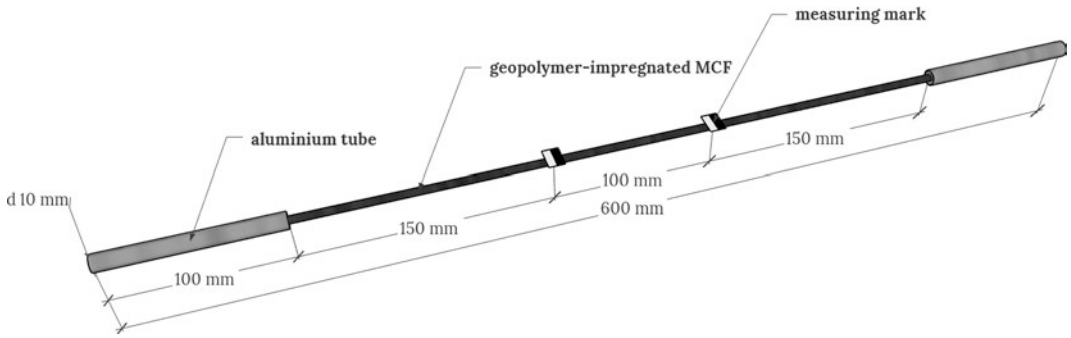

Fig. 2. Specimen for tension test.

3. Results and discussion

3.1. Temperature profile

Since the reaction kinetics of the exothermic geopolymerisation strongly depend on the curing temperature, a crucial influence on the hardening behaviour of the matrix material can be found. Several authors reported 60 °C to 75 °C as the optimal range for the curing temperature to achieve the best mechanical performance of geopolymers [17,52-55]. Therefore, the heating temperature of the yarns was monitored for the entire duration of curing. For the three different applied voltages within 2 h of treatment, the corresponding temperature developments are shown in Fig. 3. According to Joule's first law, the emitted heat depends mainly on the Amperage (A) resulting from the voltage; cf. Eq. (2). Thus, an applied voltage of 30 V results in the highest curing temperature with the steepest rate increase. Note that after five minutes a maximum temperature of 230 °C is reached at this voltage, which required the abortion of the experiment to protect the equipment from any damage. At 15 V the curve shows a short but steep increase in temperature, followed by a relatively constant temperature range between 65 °C and 70 °C, induced at an amperage of about 1.6 A. Note: After 2 h of curing, the electrical resistance decreased from 19.6 Ω to 12 Ω due to the evaporation of the insulating water film around the fibre surface [56]. The lowest voltage of 7.5 V results in a smaller, but considerable temperature rise to 50 °C, representing a maximum temperature difference of 30 K. As can be seen from all curves, the specimens reach their maximum temperature very rapidly and maintain themselves constant at the target temperature, showing that the suggested method can be considered as an efficient alternative to conventional oven curing. Moreover, the temperature curves provide a possible explanation for the strength development of the metakaolin-based, mineral-impregnated, carbon-fibre yarns, since several studies have dealt with the influence of the curing temperature on the structural development of geopolymers [16,17,52].

3.2. Flexural strength

Fig. 4 depicts the flexural strengths of the MCF tested immediately after thermal curing by Joule heating. Depending on the applied voltages and curing times, distinct flexural strengths could be reached. With extended curing duration, the MCF show higher flexural strengths due to a higher degree of geopolymerisation [16,17,52,57].

The samples thermally activated with 15 V reach the highest flexural strength after 2 h, since in particular this temperature range accelerates the geopolymerisation significantly. A mean flexural strength of 612 MPa is observed, which is 34 % higher than the flexural strength of similar geopolymer-impregnated MCF thermally cured in the oven at 75 °C for 8 h (454 MPa), reported in a previous study by the authors [23]. This is caused not only by the faster setting of the matrix but also by the distinct viscosities of the matrices. Even after a treatment duration of 15 min only, moderate flexural strength of 271 MPa could be reached.

At 30 V, the flexural strength increases up to a curing duration of one hour with a maximum of 317 MPa. However, with the extended curing to 2 h, the flexural strength decreases again, due to the formation of a more porous matrix microstructure derived from the intensive water evaporation at high temperature [17,54,58]; see also Section 3.3.

Due to the relatively low temperature at 7.5 V, those specimens did not form solidified structure within the first 90 min and could accordingly not be tested at that stage; cf. Fig. 3. After 2 h, they only reached a relatively low flexural strength of 23.5 MPa.

Fig. 5 shows representative flexural stress–deflection curves of the specimens cured for 2 h at their respective voltages. The differentially applied voltages resulted in distinct differences in the bending behaviour of MCF. The specimens cured at 15 V exhibit an initial linear elastic behaviour followed by a sudden drop in flexural stress when reaching the stress peak, thus demonstrating pronouncedly brittle behaviour of the MCF. Since unreinforced GPs are brittle by nature, it is believed that the moderate treatment with 15 V accelerates the formation of a denser and homogenous matrix microstructure, which demonstrates good

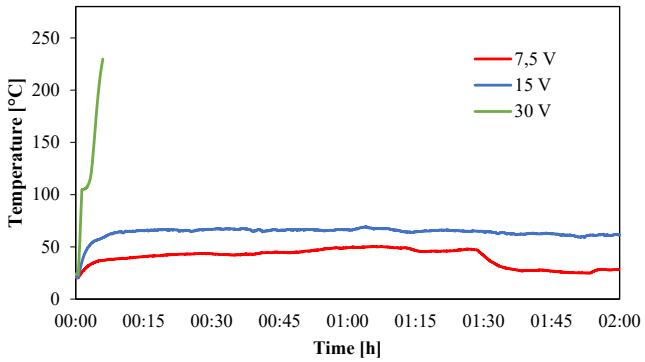

Fig. 3. Temperature profile for MCF depending on the applied voltage.

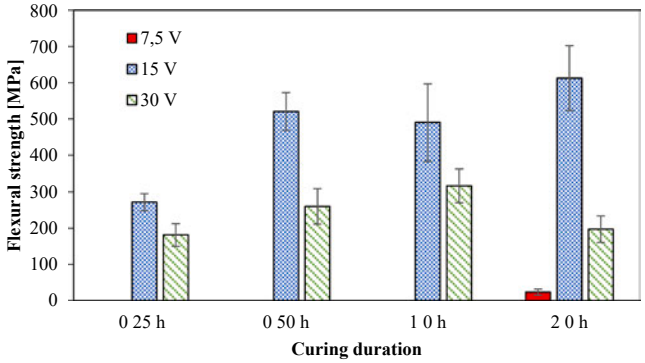

Fig. 4. Flexural strength of MCF tested immediately after curing.

Final edited form was published in "Composites : Part A, Applied science and manufacturing" 153,106750. ISSN: 1359-835X
https://doi.org/10.1016/j.compositesa.2021.106750

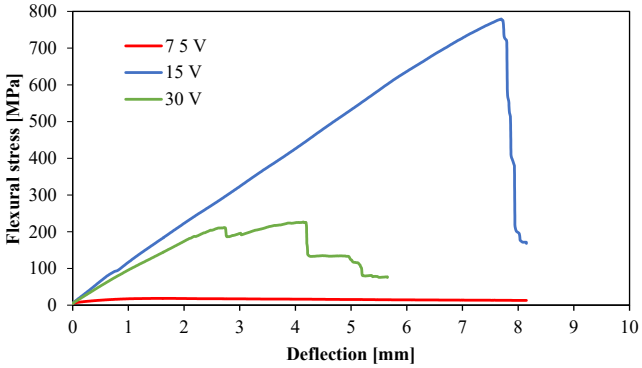

Fig. 5. Representative stress–deflection curves for MCF tested after 2 h of curing.

bridging between individual filaments and therewith more evenly distributed stress within the bundle. This assumption is supported by the observation in ESEM, showing a homogenous dense geopolymer microstructure; see Fig. 11.

In contrast, a voltage of 30 V leads to several drops in the stress–deflection curves after reaching the peak. These drops can be attributed to premature crack formations in the matrix and the sliding of filaments, indicating a less reacted microstructure and a weaker bond between filaments and matrix. The cross-section and fracture surface observation of MCF in ESEM (see Fig. 11e) demonstrated a very inhomogeneous matrix microstructure with a high number of large pores, which cause stress concentration at their edges and, thus, premature failure under bending.

Considering all failure behaviours observed, it can be concluded that the MCF cured at 15 V and 30 V showed in the samples' compression zones predominant damage and failure processes in the form of buckled, fractured, and delaminated fibres. For the samples cured at 15 V for 2 h, only a few specimens showed damages on the side under tension.

The flexural strengths of MCF cured at 15 V at different ages are illustrated in Fig. 6. Comparing the flexural strengths at an early age and after an additional storing time of 28 days, a decrease can be observed with further Joule heating; see Fig. 6. While for a curing time of 30 min a decrease of about 12% was observed, a duration of two hours resulted in a reduction of the flexural strength of 23%. This reduction was also found for oven-cured GP matrices [23] and is explained by the reorganization and ongoing geopolymerisation of the matrix microstructure, resulting in the slightly increased porosity of the samples [17]; see also Fig. 8.

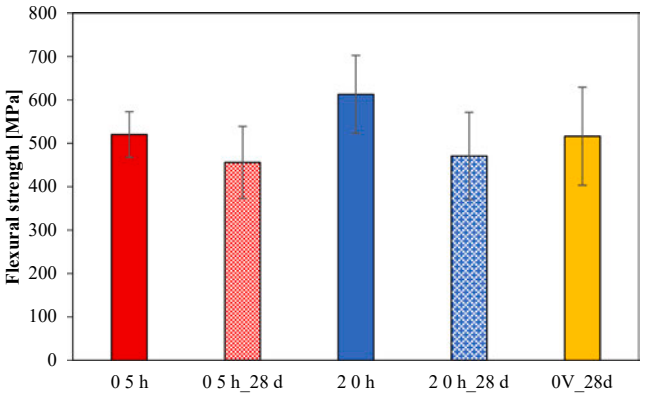

Fig. 6. Comparison of flexural strengths of MCF treated at 15 V and tested immediately after curing for 0.5 h and 2 h and after 28 d of curing. 0V_28d stands for the reference produced without curing and tested at an age of 28 days.

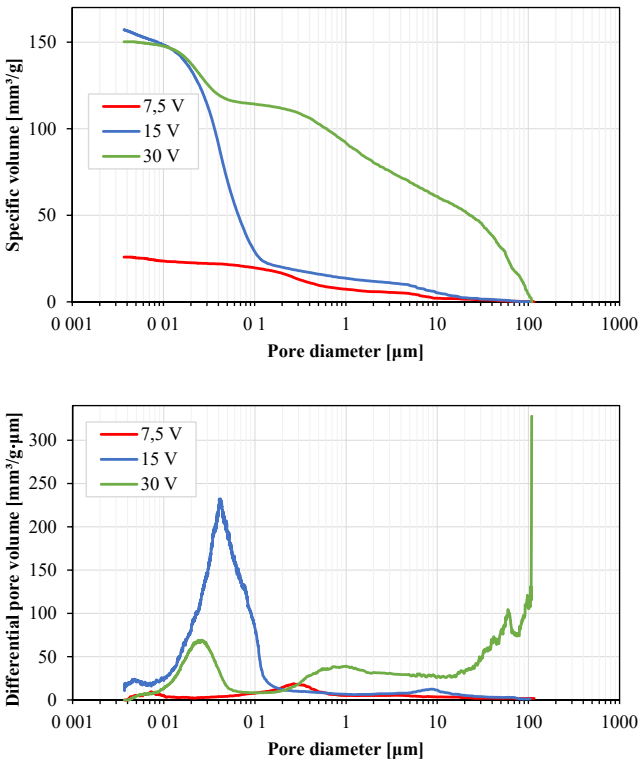

Fig. 7. Cumulative pore volume (top) and pore-size distribution (bottom) in the geopolymer MCF after curing at different voltages for 2 h.

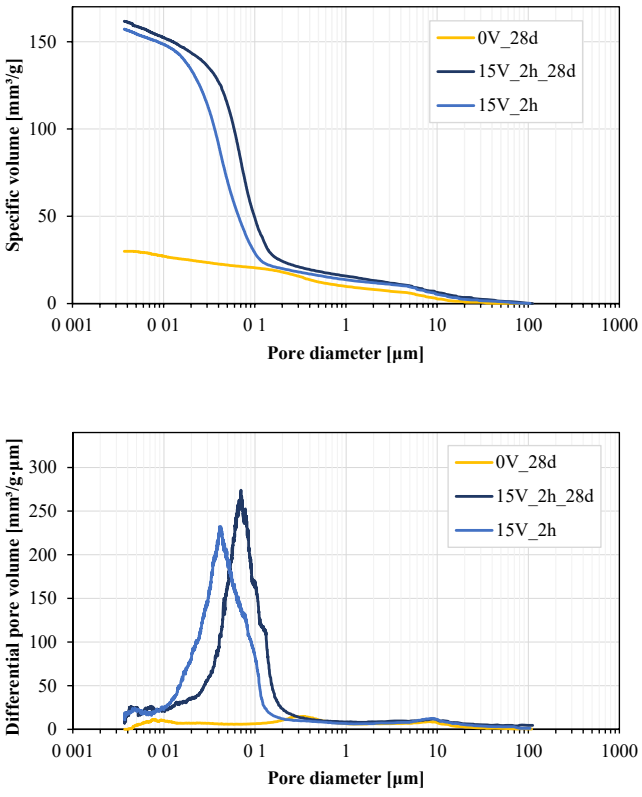

Fig. 8. Cumulative pore volume (top) and pore-size distribution (bottom) in the geopolymer MCF at an age of 28 days (0 V and 15V_2h) and after 2 h of curing.

Final edited form was published in "Composites : Part A, Applied science and manufacturing" 153,106750. ISSN: 1359-835X
https://doi.org/10.1016/j.compositesa.2021.106750

3.3. Morphological analysis

The morphological analysis confirms the distinct differences in the degree of geopolymerisation obtained and the resulting mechanical properties due to the different applied Joule heating parameters.

The MIP results show that the different curing temperatures cause distinct regimes of porosity in the samples investigated, in both cumulative pore volume and pore-size distribution; see Fig. 7. Note that the 7.5 V-treated specimens might be not appropriate to compare directly with the other two parameters due to its delayed setting.

The MCF cured at 15 V for 2 h exhibits the highest number of nano- and *meso*-sized pores, i.e., those with a nominal diameter of 3–10 nm and 10–50 nm, respectively, followed by the specimens treated at 30 V and finally at 7.5 V; see Fig. 7 and Table 4. Apparently, a more homogeneous and denser matrix can be obtained by applying lower voltages due to a slower chemical reaction process and less moisture loss during heating. That means a gradual filling of the pores and cavities between unreacted particles with aluminosilicate gel [17]. By filling these interparticle voids [59], the amount of *meso*-sized pores (3–50 nm) increases, indicating a higher degree of geopolymerisation, as seen in the 15 V-test series.

At higher applied voltages a higher total porosity was observed, especially in the form of macro-sized (50–200 nm) and even larger (>200 nm) pores. Note that very large pores, as seen in ESEM and μCT analysis are even beyond the maximum measurement range of 100 μm; see Fig. 11 and Fig. 13. This excessive pore formation is traced back to the rapid evaporation of water during thermal curing [53] and to insufficient reaction. Rapid geopolymerisation at high temperature causes sealing of the partially reacted metakaolin particles [17,52], which hinders their full dissolution. This can be seen in the microscopic image for the 30 V specimen, where the rapidly risen high temperature resulted in a loose structure of partially unreacted metakaolin particles surrounded by a geopolymer gel shell; see Fig. 11f [17,52]. These large pores act as defects and hence cause the considerably lower flexural strength of the MCF cured at 30 V; see Fig. 5.

After 28 days, the porosity of the MCF was slightly changed, as representatively shown for samples cured at 15 V; see Fig. 8 and Table 4. Note that for a better understanding also the 28-day reference without any applied voltage is given. This particular sample shows similar flexural properties as samples cured with 15 V and a superior tensile strength; see Fig. 6 and Table 5. With 5.8 % of pore volume, it also possesses a very dense matrix, as is also visible in the ESEM images in Fig. 12. Apparently, without accelerated curing the reactive geopolymer suspension formed a very dense microstructure [17]. The applied internal heating yielded a pronounced nano- and micro-porosity, which changed somewhat further after the thermal process. While the number of nanopores (3–10 nm) and larger pores (>200 nm) were in the same range, at an age of 28 days the amount of mesopores decreased while the amount of macropores increases in comparison to the state immediately after curing; see Fig. 8 and Table 4. This indicates a reorganization and further geopolymerisation of the matrix and explains the slightly inferior flexural and tensile performance of MCF after 28 days' storing; see Fig. 6 and Table 5.

Table 4
Porosity of geopolymer-impregnated MCF after 2 h of curing depending on various voltages.

Sample	Nanopores (3–10 nm) [Vol.-%]	Mesopores (10–50 nm) [Vol.-%]	Macropores (50–200 nm) [Vol.-%]	Larger Pores (>200 nm) [Vol.-%]	Porosity by Hg-Intrusion [Vol.-%]
0 V (28 d)	0.53	1.04	0.61	3.65	5.84
7.5 V	0.49	0.45	0.87	3.58	5.39
15 V	1.38	13.90	6.49	3.27	25.07
15 V (28 d)	1.55	7.809	13.12	4.25	26.74
30 V	0.42	5.25	0.64	18.7	25.01

To verify the influence of Joule heating on the MCF microstructure and to assess the fibre weight content, thermogravimetric analysis (TGA) was carried out. Fig. 9 presents the results for MCF treated for 2 h at 7.5 V, 15 V, and 30 V, respectively. All samples show clear differences in their thermal decomposition behaviour, and particular temperature ranges can be observed. The first significant weight loss can be seen in the range between approx. 60 °C and 200 °C, which can be traced back to the loss of both physically and chemically bonded water [23,60]. At this particular temperature range the DTG-curves show a significantly higher weight loss for MCF cured at lower voltages (7.5 V and 15 V), caused by higher amounts of freely evaporable and chemically bound water from the geopolymer-matrix [23,61] being evaporated. Besides the high amount of water, high amounts of unreacted $Al(OH)_3$ and $Si(OH)_4$ are likely still to exist in the case of 7.5 V. For the 30 V-series, a smaller degree of maximum weight loss was to be seen due to less pronounced geopolymerisation since a great deal of physical and chemical bound water was already evaporated during the curing process at high temperatures of above 200 °C. Above 300 °C, the weight loss can also be ascribed to the dehydroxylation of the hydroxyl-groups [62].

The second prominent weight-loss peak is mainly governed by the oxidation of the carbon fibres in the range between 450 °C and 650 °C. For the MCF cured at 30 V, this peak appears at slightly lower temperatures. On the one hand, this can be explained by the porous and less thermally stable matrix microstructure, which is not able to protect the yarn from oxidizing. On the other hand, it might also indicate some damage to CF filaments due to the applied high voltage, which is to be elucidated in a future study.

At an age of 28 days, similar behaviour could be observed; see Fig. 10. For the 15V_2h_28d-sample, the CF decomposition peak (~572 °C) appeared slightly earlier since the higher amount of macropores expose the carbon fibres more to the oxidative environment, in comparison to the denser matrix observed just after thermal curing. For the uncured reference samples, a pronounced weight loss is seen at around 144 °C, which is due to the excessive loss of chemically and physically bound water from the dense geopolymer matrix. It also shows a high temperature at the second weight loss peak (599 °C) corresponding to CF oxidation, indicating good thermal protection of the CF yarn by the relatively dense matrix. Based on the TGA curves the carbon-fibre weight content lies between 17.8 % and 19.8 %, respectively, corresponding to a volume content between 16.6 % and 18.5 %.

ESEM images confirm the results of MIP and TGA. In Fig. 11, the cross-sections are shown for the MCF cured at 7.5 V, 15 V and 30 V, exhibiting dramatic differences with regard to pores and cracks. The lower the voltage is, the denser the matrix. The composite treated at 30 V showed a high number of huge voids (black areas) over the whole cross-section. According to the μCT analysis, those voids were spread throughout the entire specimen; see Fig. 13. Moreover, the high curing temperature caused by higher voltages resulted also in the formation of more radial cracks in the matrix microstructure, likely due to excessive water evaporation and pronounced shrinkage during heating. These cracks probably also impair the mechanical performance of the MCF.

Considering the morphology of the MCF in fibre direction, it can be seen that the high temperatures caused the formation of a very inhomogeneous, loosely packed matrix due to fast water evaporation from the GP suspension; see Fig. 11, right column. For the specimens treated at 30 V, a high amount of small, partially reacted particles can be found; see Fig. 11f. As explained above, the high temperatures can induce the formation of solid phases on the particle surfaces, leading to a deceleration of the geopolymerisation reaction [17,52]. In contrast, a very dense matrix was formed in the case of curing with 7.5 V, with only few unreacted metakaolin particles and hardly any defects. The sample cured at 15 V possesses several voids, likely caused by dissolving of the metakaolin particles; cf. Fig. 11 b) and d). After 28 days' storage, the

Final edited form was published in "Composites : Part A, Applied science and manufacturing" 153,106750. ISSN: 1359-835X
https://doi.org/10.1016/j.compositesa.2021.106750

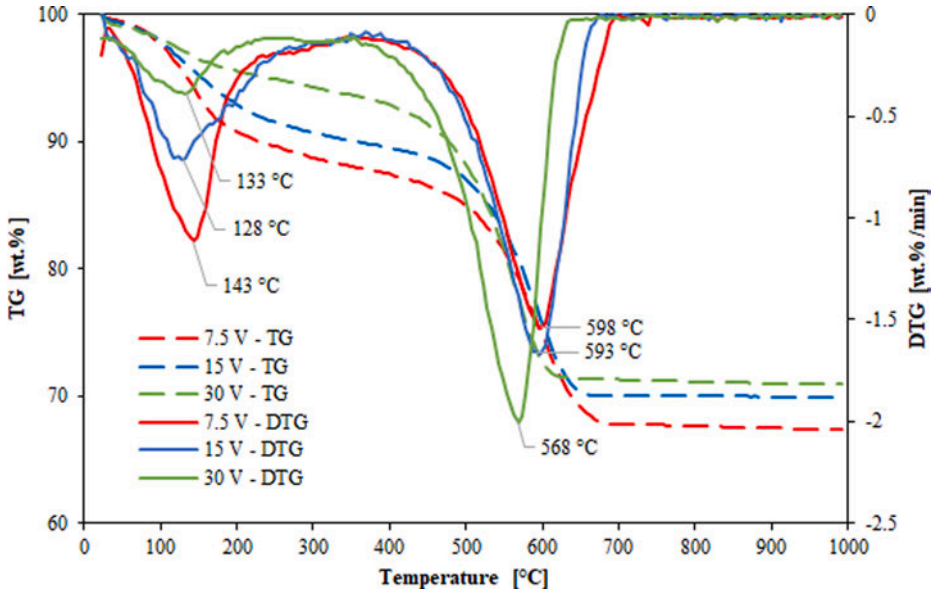

Fig. 9. TG/DTG curves for the geopolymer-MCF cured at different voltages after 2 h.

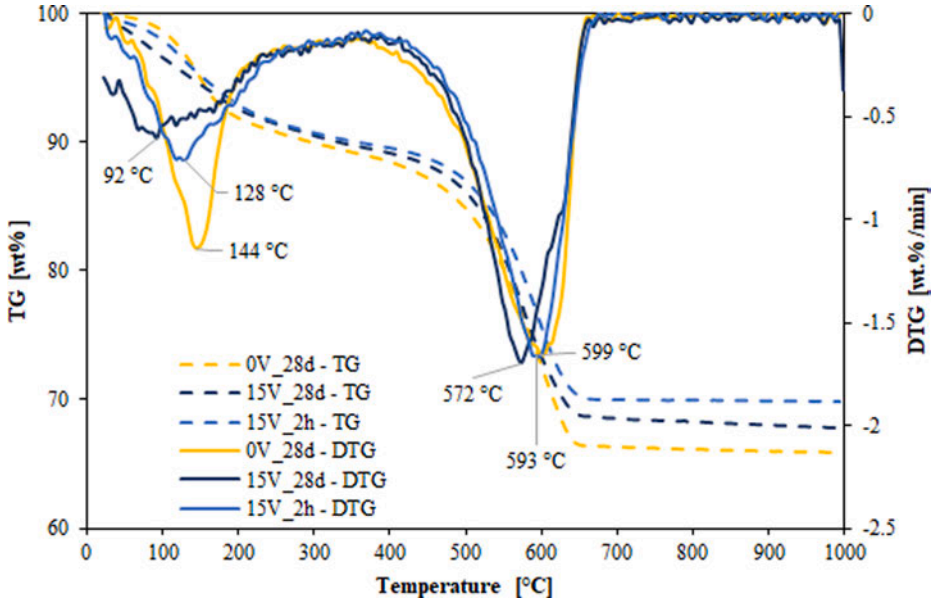

Fig. 10. TG/DTG curves for the geopolymer-MCF, 0 V and 15 V_2h, at an age of 28 days and after 2 h.

number of such voids significantly increased due to the lack of water caused by the thermal curing of the MCF; see Fig. 12a. Compared to this, the untreated reference had an extremely dense and homogenous matrix showing scarcely any voids. This is in line with the results of MIP above, indicating a high degree of geopolymerisation facilitated by the higher amount of water compared to the treated samples. Only a few cracks can be seen, which may even have been caused in preparing of the sample.

The µCT scans (Fig. 13) captured in fibre direction show the structure of the samples depending on their density, presented as differences in grey values. The scans corroborate a denser microstructure (grey) of the metakaolin-based matrix for the MCF cured at 15 V, having merely several small pores inside. The samples thermally activated at 30 V show in contrast enormous areas with low density (black) standing for voids. These areas extend throughout the entire sample. In the case of voids, these defects are caused by water evaporation induced by high temperatures, as discussed above.

3.4. Uniaxial tension behaviour

The uniaxial tension behaviour of the MCF cured at 15 V for 2 h was determined at ages of 2 d and 28 d; see Table 5. All MCF exhibit outstanding yarn tensile strengths, which are in the range of conventional CFRP reinforcements [63]. After 2 h of curing, a tensile strength of 2800 MPa was measured at 1.1 % elongation at break, while the modulus of elasticity was 265 GPa. The values for the MCF cured for 2 h with 15 V were in the same range as the geopolymer-based MCF thermally cured in the oven at 75 °C [23].

However, at an age of 28 days the thermally cured MCF exhibited a slightly lower tensile strength of 2367 MPa as well as a lower modulus of elasticity of 236 GPa; see Table 5. This is explained by further formations of voids due to the ongoing geopolymerisation as well as by the evaporation of pore water and possibly microcracks resulting from autogenous and drying shrinkage; see Fig. 8 [64,65]. The drying shrinkage is strongly related to the size of the pores, which influence the diffusion

"Final edited form was published in "Composites : Part A, Applied science and manufacturing" Vol: 153,106750. ISSN: 1359-835X
https://doi.org/10.1016/j.compositesa.2021.106750"

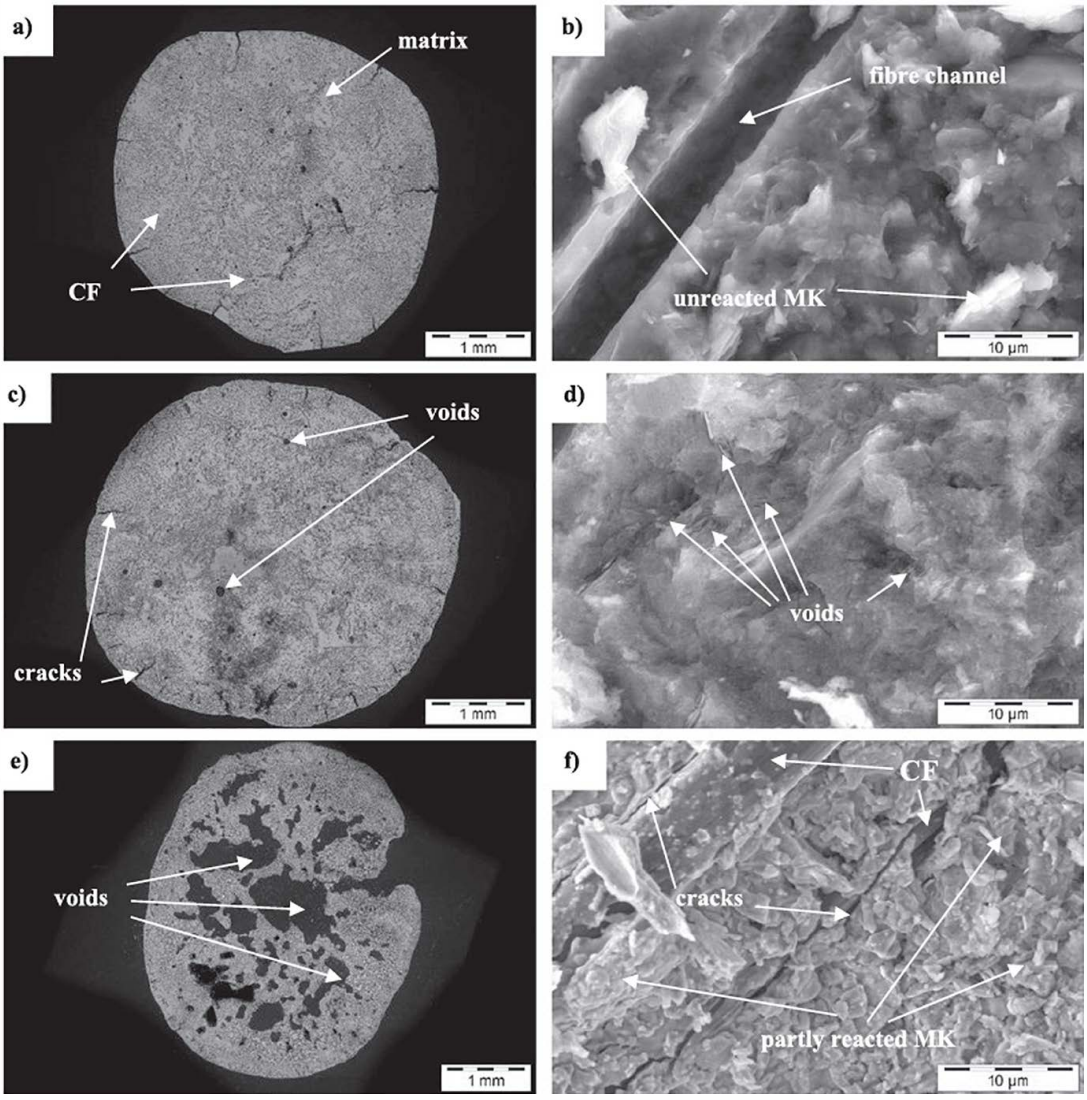

Fig. 11. ESEM-images of geopolymer MCF cured at different voltages for 2 h: a), b) 7.5 V; c), d) 15 V and e), f) 30 V.

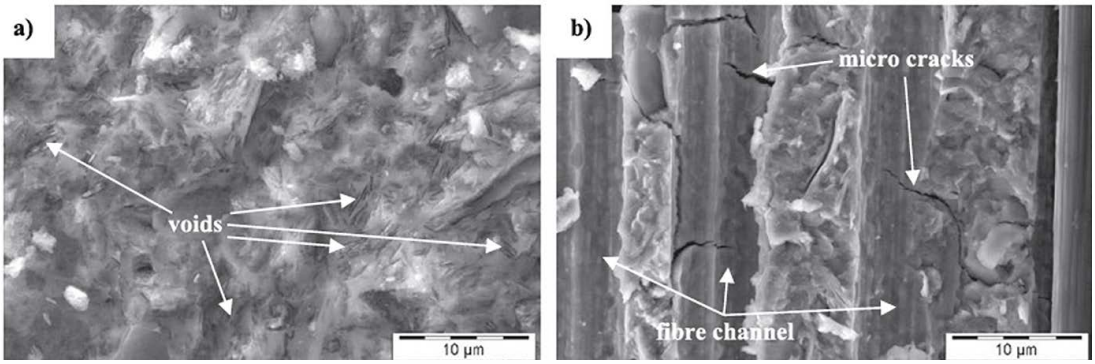

Fig. 12. ESEM-images of geopolymer MCF at the age of 28 days: a) 15V 2h; b) 0 V.

process of pore water to the external environment [66].

The untreated reference MCF showed the highest tensile strength of 3122 MPa, but a slightly lower Young's modulus of 221 GPa; see Table 5. This indicates that curing at room temperature yielded the most homogenous GP microstructure as can be also seen in the results from MIP, see Fig. 8 and Table 4. Only a very small number of pores could be detected for the untreated reference at an age of 28 days. This is finally also expressed in the smallest standard deviation of all the test results. The failure mechanism of the reference samples is mainly governed by fibre rupture, confirming the excellent force transfer between the individual filaments.

Apart from fibre rupture, interlaminar shear failure can be also observed for the modified samples, indicating insufficient shear force transfer between outer and inner filaments as the voids in the

"Final edited form was published in "Composites : Part A, Applied science and manufacturing" Vol: 153,106750. ISSN: 1359-835X
https://doi.org/10.1016/j.compositesa.2021.106750"

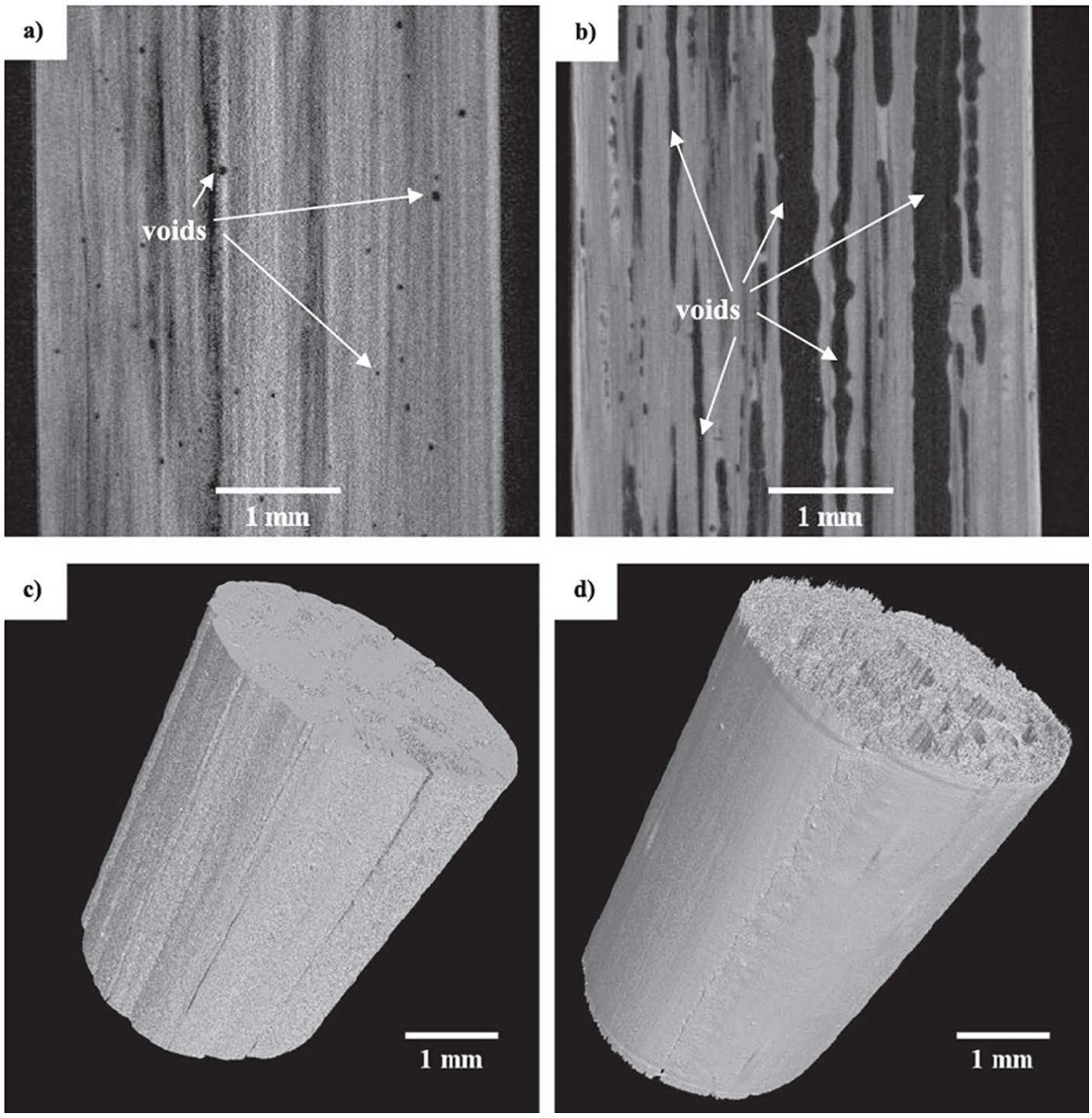

Fig. 13. µCT-Scans of MCF cured at a), c) 15 V and b), d) 30 V for 2 h.

Table 5
Tensile strength and Young's modulus of chosen samples; standard deviation given in brackets

Sample	Tensile strength [MPa]	Young's modulus [GPa]
2h 2d	2800 (216)	265 (26)
2h_28d	2367 (242)	236 (25)
Ref_28d	3122 (107)	221 (17)

geopolymer matrix reduce its bridging effect. Nevertheless, the tensile properties obtained are still in the range of conventional CFRP reinforcements [63].

3.5. Manufacture of flexible reinforcement shapes

A desirable application of Joule heating of freshly impregnated MCF is the flexible out-of-oven production in a variety of shapes. To demonstrate the feasibility of this method, MCF were brought into shape in the fresh state and then thermo-electrically cured with an appropriate voltage in the range of 15 V, to obtain amperages on similar levels. Thus, it was possible to produce 3D-objects in different shapes with a mere 15 min of curing with 15 V; see Fig. 14.

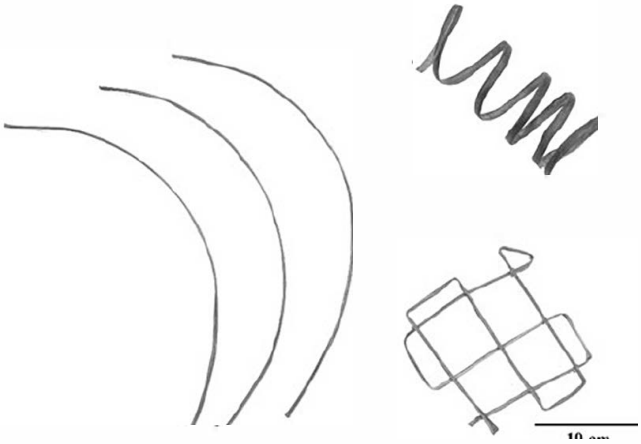

Fig. 14. MCF with different shapes manufactured using Ohmic heating.

Nonetheless, it is noteworthy that for producing flexible MCF reinforcements via Joule heating in practice, some issues still need solving. Especially when fabricating textile structures, the contact at the yarn

crossing points influences the current conduction and therefore the heating of the whole sample. This difficulty can be solved, e.g., by installing insulating spacers. Moreover, to heat up reinforcement over several meters the applications of the electrodes need to be mastered in an automated way to achieve a stable and uniform current throughout the entire sample reliably. By mastering these challenges, it will be possible to get a large variety of two- and three-dimensional reinforcements after only a few minutes of curing.

4. Summary

The application of metakaolin-based geopolymer binders for impregnating CF yarns is a new approach that enables improved thermal stability in concrete reinforcements made with carbon fibres. Since geopolymerisation significantly accelerated at elevated temperatures, it is favourable to activate the geopolymer-impregnated CF yarns thermally. Conventional methods are oven curing, steam curing or the use of an autoclave. However, these methods are inefficient in terms of energy consumption and often not applicable for larger three-dimensional shapes.

To optimize the thermal treatment of geopolymer-based MCF, this research focused on the use of the Joule heating effect on curing the carbon-fibre composites under a combination of different parameters. After thermal treatment at 7.5 V, 15 V and 30 V for 0.25 h, 0.50 h, 1 h and 2 h, the mechanical and morphological properties of the MCF were investigated. Due to the differential heating of the samples caused at such particular voltages, the setting and strength development proceeded at different rates. It can be seen that the specimens cured at 15 V showed the fastest gain in strength with the highest flexural strength of the test series. After only 15 min of curing, maximum flexural stresses of 271 MPa could be measured. The flexural strength further increased to 612 MPa after 2 h of curing. Hence, it is concluded that for the parameters under investigation the best results could be achieved by the combination of 15 V for a curing duration of 2 h for a sample length of 1.0 m. The composite reached a tensile strength and a modulus of elasticity of 2800 MPa and 265 GPa, respectively. However, the morphological analyses revealed a negative impact of the Joule-heating on the formation of a dense and homogenized microstructure, to some extent due to the accelerated reaction and the unavoidable evaporation of water from the metakaolin-based binder. By controlling the environmental humidity and the formation of the unavoidable pore structure, the density of the microstructure could be improved.

In addition to the superior mechanical behaviour of the geopolymer-impregnated carbon-fibre composites, the use of Joule heating presents high potential in manufacturing flexible, shaped reinforcements including unidirectional yarns, 2D or 3D textiles within very short curing periods, as shown.

In summary, Ohmic heating is a highly promising approach for the thermal activation of mineral-impregnated, carbon-fibre yarns based on geopolymers. It enables fast and energy-efficient curing with a broad range of producible reinforcement shapes due to the uniform heating of the composites over their entire cross section.

CRediT authorship contribution statement

Dominik Junger: Conceptualization, Methodology, Validation, Investigation, Data curation, Formal analysis, Writing – original draft, Writing – review & editing, Visualization. **Marco Liebscher:** Conceptualization, Methodology, Validation, Investigation, Writing – original draft, Writing – review & editing, Supervision, Project administration. **Jitong Zhao:** Methodology, Investigation, Validation, Writing – review & editing, Supervision. **Viktor Mechtcherine:** Resources, Supervision.

Declaration of Competing Interest

The authors declare that they have no known competing financial interests or personal relationships that could have appeared to influence the work reported in this paper.

References

[1] Scheerer S. Was ist Textilbeton?: Eine kurze Einführung in das Thema. Beton-Stahlbetonbau 2015;110(S1):4–7. https://doi.org/10.1002/best.201400104.
[2] Mechtcherine V, Michel A, Liebscher M, Schneider K, Großmann C. Neue Carbonfaserbewehrung für digitalen automatisierten Betonbau. Beton-Stahlbetonbau 2019;114(12):947–55. https://doi.org/10.1002/best.201900058.
[3] Cherif C, editor. Textile Werkstoffe für den Leichtbau. Berlin, Heidelberg: Springer Berlin Heidelberg; 2011.
[4] Schumann A, May M, Curbach M. Carbonstabe im Bauwesen: Teil 1: Grundlegende Materialcharakteristiken. Beton- Stahlbetonbau 2018;113(12):868–76. https://doi.org/10.1002/best.201800077.
[5] Kapsalis P, El Kadi M, Vervloet J, De Munck M, Wastiels J, Triantafillou T, et al. Thermomechanical Behavior of Textile Reinforced Cementitious Composites Subjected to Fire. Appl Sci 2019;9(4):747. https://doi.org/10.3390/app9040747.
[6] Silva FdA, Butler M, Hempel S, Toledo Filho RD, Mechtcherine V. Effects of elevated temperatures on the interface properties of carbon textile-reinforced concrete. Cem Concr Compos 2014;48:26–34. https://doi.org/10.1016/j.cemconcomp.2014.01.007.
[7] Katz A, Berman N, Bank LC. Effect of High Temperature on Bond Strength of FRP Rebars. J Compos Constr 1999;3(2):73–81. https://doi.org/10.1061/(ASCE)1090-0268(1999)3:2(73).
[8] Bazli M, Abolfazli M. Mechanical Properties of Fibre Reinforced Polymers under Elevated Temperatures: An Overview. Polymers 2020;12:2600. https://doi.org/10.3390/polym12112600.
[9] Nguyen KTQ, Navaratnam S, Mendis P, Zhang K, Barnett J, Wang H. Fire safety of composites in prefabricated buildings: From fibre reinforced polymer to textile reinforced concrete. Compos B Eng 2020;187:107815. https://doi.org/10.1016/j.compositesb:2020.107815.
[10] Hamad RJA, Megat Johari MA, Haddad RH. Mechanical properties and bond characteristics of different fiber reinforced polymer rebars at elevated temperatures. Constr Build Mater 2017;142:521–35. https://doi.org/10.1016/j.conbuildmat.2017.03.113.
[11] Katz A, Berman N. Modeling the effect of high temperature on the bond of FRP reinforcing bars to concrete. Cem Concr Compos 2000;22(6):433–43. https://doi.org/10.1016/S0958-9465(00)00043-3.
[12] Schneider K, Lieboldt M, Liebscher M, Frohlich M, Hempel S, Butler M, et al. Mineral-Based Coating of Plasma-Treated Carbon Fibre Rovings for Carbon Concrete Composites with Enhanced Mechanical Performance. Materials 2017;10(4):360. https://doi.org/10.3390/ma10040360.
[13] Schneider K, Michel A, Liebscher M, Terreri L, Hempel S, Mechtcherine V. Mineral-impregnated carbon fibre reinforcement for high temperature resistance of thin-walled concrete structures. Cem Concr Compos 2019;97:68–77. https://doi.org/10.1016/j.cemconcomp.2018.12.006.
[14] Mechtcherine V, Michel A, Liebscher M, Schneider K, Großmann C. Mineral-impregnated carbon fiber composites as novel reinforcement for concrete construction: Material and automation perspectives. Autom Constr 2020;110:103002. https://doi.org/10.1016/j.autcon.2019.103002.
[15] Mechtcherine V, Michel A, Liebscher M, Schmeier T. Extrusion-Based Additive Manufacturing with Carbon Reinforced Concrete: Concept and Feasibility Study. Materials 2020;13:2568. https://doi.org/10.3390/ma13112568.
[16] Muniz-Villarreal MS, Manzano-Ramírez A, Sampieri-Bulbarela S, Gasca-Tirado JR, Reyes-Araiza JL, Rubio-Ávalos JC, et al. The effect of temperature on the geopolymerization process of a metakaolin-based geopolymer. Mater Lett 2011;65(6):995–8. https://doi.org/10.1016/j.matlet.2010.12.049.
[17] Rovnaník P. Effect of curing temperature on the development of hard structure of metakaolin-based geopolymer. Constr Build Mater 2010;24(7):1176–83. https://doi.org/10.1016/j.conbuildmat.2009.12.023.
[18] Shaikh F, Haque S. Behaviour of Carbon and Basalt Fibres Reinforced Fly Ash Geopolymer at Elevated Temperatures. Int J Concr Struct Mater 2018;12:35. https://doi.org/10.1186/s40069-018-0267-2.
[19] Zhang H, Kodur V, Cao L, Qi S. Fiber Reinforced Geopolymers for Fire Resistance Applications. Procedia Eng 2014;71:153–8. https://doi.org/10.1016/j.proeng.2014.04.022.
[20] Pernica D, Reis PNB, Ferreira JAM, Louda P. Effect of test conditions on the bending strength of a geopolymer-reinforced composite. J Mater Sci 2010;45(3):744–9. https://doi.org/10.1007/s10853-009-3994-6.
[21] Doan T, Louda P, Kroisova D, Bortnovsky O, Thang N. In: Advances in Composite Materials - Analysis of Natural and Man-Made Materials. InTech; 2011. https://doi.org/10.5772/17933.
[22] Tran H, Kroisová D, Louda P, Bortnovsky O, Bezucha P. Effect of curing temperature on flexural properties of silica-based geopolymer-carbon reinforced composite. J Achievements Manuf Eng 2009;37.
[23] Zhao J, Liebscher M, Michel A, Junger D, Trindade ACC, de Andrade Silva F, et al. Development and testing of fast curing, mineral-impregnated carbon fiber (MCF) reinforcements based on metakaolin-made geopolymers. Cem Concr Compos 2021;116:103898. https://doi.org/10.1016/j.cemconcomp.2020.103898.
[24] Narayanan A, Shanmugasundaram P. An Experimental Investigation on Flyash-based Geopolymer Mortar under different curing regime for Thermal Analysis. Energy Build 2017;138:539–45. https://doi.org/10.1016/j.enbuild.2016.12.079.

[25] Srinivasan K, Sivakumar A. Chemical activation and curing regime of geopolymer concretes. In: Proceedings of the Institution of Civil Engineers - Construction Materials 2015;168:24–34. Doi: 10.1680/coma.13.00024.
[26] He P, Jia D, Lin T, Wang M, Zhou Yu. Effects of high-temperature heat treatment on the mechanical properties of unidirectional carbon fiber reinforced geopolymer composites. Ceram Int 2010;36(4):1447–53. https://doi.org/10.1016/j.ceramint.2010.02.012.
[27] Athanasopoulos N, Sotiriadis G, Kostopoulos V. A study on the effect of Joule-heating during the liquid composite molding (LCM) process and on the curing of CFRP composite laminates. In: 10th International Conference on Flow Processes in Composite Materials (FPCM10), Ascona, Switzerland: 2010.
[28] Kovtun M, Ziolkowski M, Shekhovtsova J, Kearsley E. Direct electric curing of alkali-activated fly ash concretes: a tool for wider utilization of fly ashes. J Cleaner Prod 2016;133:220–7. https://doi.org/10.1016/j.jclepro.2016.05.098.
[29] Ziolkowski M, Kovtun M. Confined-Direct Electric Curing of NaOH-activated fly ash based brick mixtures under free drainage conditions: Part 1. Factorial experimental design. Constr Build Mater 2017;155:1050–62. https://doi.org/10.1016/j.conbuildmat.2017.08.135.
[30] Ziolkowski M, Kovtun M. Confined-Direct Electric Curing of NaOH-activated fly ash based brick mixtures under free drainage conditions: Part 2. Confined-DEC versus oven curing. Constr Build Mater 2018;176:452–61. https://doi.org/10.1016/j.conbuildmat.2018.05.041.
[31] Cai J, Li X, Tan J, Vandevyvere B. Fly ash-based geopolymer with self-heating capacity for accelerated curing. J Cleaner Prod 2020;261:121119. https://doi.org/10.1016/j.jclepro.2020.121119.
[32] Tian W, Wang M, Liu Y, Wang W. Ohmic heating curing of high content fly ash blended cement-based composites towards sustainable green construction materials used in severe cold region. J Cleaner Prod 2020;276:123300. https://doi.org/10.1016/j.jclepro.2020.123300.
[33] Gomis J, Galao O, Gomis V, Zornoza E, Garcés P. Self-heating and deicing conductive cement. Experimental study and modeling. Constr Build Mater 2015;75:442–9. https://doi.org/10.1016/j.conbuildmat.2014.11.042.
[34] Sassani A, Arabzadeh A, Ceylan H, Kim S, Sadati SMS, Gopalakrishnan K, et al. Carbon fiber-based electrically conductive concrete for salt-free deicing of pavements. J Cleaner Prod 2018;203:799–809. https://doi.org/10.1016/j.jclepro.2018.08.315.
[35] Hambach M, Moller H, Neumann T, Volkmer D. Carbon fibre reinforced cement-based composites as smart floor heating materials. Compos B Eng 2016;90:465–70. https://doi.org/10.1016/j.compositesb.2016.01.043.
[36] Chang C, Ho M, Song G, Mo Y-L, Li H. A feasibility study of self-heating concrete utilizing carbon nanofiber heating elements. Smart Mater Struct 2009;18(12):127001. https://doi.org/10.1088/0964-1726/18/12/127001.
[37] Notani MA, Arabzadeh A, Ceylan H, Kim S, Gopalakrishnan K. Effect of Carbon-Fiber Properties on Volumetrics and Ohmic Heating of Electrically Conductive Asphalt Concrete. J Mater Civ Eng 2019;31(9):04019200. https://doi.org/10.1061/(ASCE)MT.1943-5533.0002868.
[38] Galao O, Banón L, Baeza F, Carmona J, Garcés P. Highly Conductive Carbon Fiber Reinforced Concrete for Icing Prevention and Curing. Materials 2016;9:281. https://doi.org/10.3390/ma9040281.
[39] Zhao H, Wu Z, Wang S, Zheng J, Che G. Concrete pavement deicing with carbon fiber heating wires. Cold Reg Sci Technol 2011;65(3):413–20. https://doi.org/10.1016/j.coldregions.2010.10.010.
[40] Naskar AK, Edie DD. Consolidation of Reactive Ultem®Powder-coated Carbon Fiber Tow for Space Structure Composites by Resistive Heating. J Compos Mater 2006;40(20):1871–83. https://doi.org/10.1177/0021998306061300.
[41] Sarles SA, Leo DJ. Consolidation of U-Nyte® Epoxy-Coated Carbon-Fiber Composites via Temperature-Controlled Resistive Heating. J Compos Mater 2008;42(24):2551–66. https://doi.org/10.1177/0021998308097197.
[42] Hayes SA, Lafferty AD, Altinkurt G, Wilson PR, Collinson M, Duchene P. Direct electrical cure of carbon fiber composites. Adv Manuf Polym Compos Sci 2015;1(2):112–9. https://doi.org/10.1179/2055035915Y.0000000001.
[43] Joseph C, Viney C. Electrical resistance curing of carbon-fibre/epoxy composites. Compos Sci Technol 2000;60(2):315–9. https://doi.org/10.1016/S0266-3538(99)00112-8.
[44] Fukuda H. Processing of carbon fiber reinforced plastics by means of Joule heating. Adv Compos Mater 1994;3(3):153–61. https://doi.org/10.1163/156855194X00015.
[45] Liu S, Li Y, Shen Y, Lu Y. Mechanical performance of carbon fiber/epoxy composites cured by self-resistance electric heating method. Int J Adv Manuf Technol 2019;103(9-12):3479–93. https://doi.org/10.1007/s00170-019-03707-0.
[46] Liu Yi, van Vliet T, Tao Y, Busfield JJC, Peijs T, Bilotti E, et al. Sustainable and self-regulating out-of-oven manufacturing of FRPs with integrated multifunctional capabilities. Compos Sci Technol 2020;190:108032. https://doi.org/10.1016/j.compscitech.2020.108032.
[47] Lee J, Ni X, Daso F, Xiao X, King D, Gómez JS, et al. Advanced carbon fiber composite out-of-autoclave laminate manufacture via nanostructured out-of-oven conductive curing. Compos Sci Technol 2018;166:150–9. https://doi.org/10.1016/j.compscitech.2018.02.031.
[48] Karalis G, Tzounis L, Dimos E, Mytafides CK, Liebscher M, Karydis-Messinis A, et al. Printed Single-Wall Carbon Nanotube-Based Joule Heating Devices Integrated as Functional Laminae in Advanced Composites. ACS Appl Mater Interfaces 2021;13(33):39880–93. https://doi.org/10.1021/acsami.1c10001.
[49] Zhao J, Liebscher M, Tzounis L, Mechtcherine V. Role of sizing agent on the microstructure morphology and mechanical properties of mineral-impregnated carbon-fiber (MCF) reinforcement made with geopolymers. Appl Surf Sci 2021;567:150740. https://doi.org/10.1016/j.apsusc.2021.150740.
[50] ISO 10406-1, Fibre-reinforced polymer (FRP) reinforcement of concrete — Test methods — Part 1: FRP bars and grids. 2015.
[51] Schütze E, Bielak J, Scheerer S, Hegger J, Curbach M. Einaxialer Zugversuch für Carbonbeton mit textiler Bewehrung. Beton- Stahlbetonbau 2018;113(1):33–47. https://doi.org/10.1002/best.v113.110.1002/best.201700074.
[52] Chen L, Wang Z, Wang Y, Feng J. Preparation and Properties of Alkali Activated Metakaolin-Based Geopolymer. Materials 2016;9:767. https://doi.org/10.3390/ma9090767.
[53] Aredes FGM, Campos TMB, Machado JPB, Sakane KK, Thim GP, Brunelli DD. Effect of cure temperature on the formation of metakaolinite-based geopolymer. Ceram Int 2015;41(6):7302–11. https://doi.org/10.1016/j.ceramint.2015.02.022.
[54] Bakria AMMA, Kamarudin H, BinHussain M, Nizar IK, Zarina Y, Rafiza AR. The Effect of Curing Temperature on Physical and Chemical Properties of Geopolymers. Phys Procedia 2011;22:286–91. https://doi.org/10.1016/j.phpro.2011.11.045.
[55] Kirschner AV, Harmuth H. Investigation of geopolymer binders with respect to their application for building materials. Ceram Silik 2004;48:117–20.
[56] Liebscher M, Tzounis L, Junger D, Dinh TT, Mechtcherine V. Electrical Joule heating of cementitious nanocomposites filled with multi-walled carbon nanotubes: role of filler concentration, water content, and cement age. Smart Mater Struct 2020;29(12):125019. https://doi.org/10.1088/1361-665X/abc23b.
[57] García-Mejía TA, de Lourdes Chávez-García Ma. Compressive Strength of Metakaolin-Based Geopolymers: Influence of KOH Concentration, Temperature, Time and Relative Humidity. MSA 2016;07:772–91. https://doi.org/10.4236/msa.2016.711060.
[58] Heah CY, Kamarudin H, Bakri AMMA, Binhussain M, Luqman M, Nizar IK, et al. Effect of Curing Profile on Kaolin-based Geopolymers. Phys Procedia 2011;22:305–11. https://doi.org/10.1016/j.phpro.2011.11.048.
[59] Rouquerol J, Baron G, Denoyel R, Giesche H, Groen J, Klobes P, et al. Liquid intrusion and alternative methods for the characterization of macroporous materials (IUPAC Technical Report). Pure Appl Chem 2011;84:107–36. https://doi.org/10.1351/PAC-REP-10-11-19.
[60] Chen JY, Tao S, Lei XR, Zhu XY. The Characteristics of Metakaolinite-Based Geopolymer at Different Temperature. AMM 2013;442:152–5. https://doi.org/10.4028/www.scientific.net/AMM.442.152.
[61] Bernal SA, Rodríguez ED, Mejía de Gutiérrez R, Gordillo M, Provis JL. Mechanical and thermal characterisation of geopolymers based on silicate-activated metakaolin/slag blends. J Mater Sci 2011;46(16):5477–86. https://doi.org/10.1007/s10853-011-5490-z.
[62] Caballero LR, Paiva M Das DM, Fairbairn E De MR, Toledo Filho RD. Thermal, Mechanical and Microstructural Analysis of Metakaolin Based Geopolymers. Mat Res 2019;22:e20180716. https://doi.org/10.1590/1980-5373-mr-2018-0716.
[63] Shakir Abbood I, aldeen OdaaS, Hasan KF, Jasim MA. Properties evaluation of fiber reinforced polymers and their constituent materials used in structures – A review. Mater Today: Proc 2021;43:1003–8. https://doi.org/10.1016/j.matpr.2020.07.636.
[64] Thomas RJ, Lezama D, Peethamparan S. On drying shrinkage in alkali-activated concrete: Improving dimensional stability by aging or heat-curing. Cem Concr Res 2017;91:13–23. https://doi.org/10.1016/j.cemconres.2016.10.003.
[65] Bažant ZP. Prediction of concrete creep and shrinkage: past, present and future. Nucl Eng Des 2001;203(1):27–38. https://doi.org/10.1016/S0029-5493(00)00299-5.
[66] Collins F, Sanjayan JG. Effect of pore size distribution on drying shrinking of alkali-activated slag concrete. Cem Concr Res 2000;30(9):1401–6. https://doi.org/10.1016/S0008-8846(00)00327-6.